ELSEVIER

Journal of Photochemistry and Photobiology A: Chemistry 145 (2001) 11–16

Journal of Photochemistry and Photobiology A:Chemistry

www.elsevier.com/locate/jphotochem

Preparation of Pt/TiO_2 nanocomposite thin films by pulsed laser deposition and their photoelectrochemical behaviors

Takeshi Sasaki [a,*], Naoto Koshizaki [a], Jong-Won Yoon [a], Kenneth M. Beck [b]

[a] *Nanoarchitectonics Research Center, National Institute of Advanced Industrial Science and Technology, Central 5, 1-1-1 Higashi, Tsukuba, Ibaraki 305-8565, Japan*

[b] *William R. Wiley Environmental Molecular Sciences Laboratory, Pacific Northwest National Laboratory K8-88, Richland, WA 99352, USA*

Received 3 April 2001; received in revised form 25 June 2001; accepted 4 July 2001

Abstract

Pt/TiO_2 nanocomposite films were prepared from the sintered mixture targets of Pt and TiO_2 by pulsed laser deposition. Pt/Ti atomic ratios in the deposited films are more strongly dependent on the initial content of Pt in the target than on the laser fluence. It is inferred from transmission electron microscope, X-ray photoelectron spectroscopy and X-ray diffraction analyses that as-deposited Pt/TiO_2 nanocomposite films are composed of metallic Pt nanoparticles with a diameter of about 30 nm and an amorphous TiO_2 matrix, which are crystallized into the dominant crystal structure of the anatase phase after the heating at 600°C. The optical bandgap of Pt/TiO_2 nanocomposite films was less than that of the pure TiO_2 film and photoluminescence emission was observed between 680 and 800 nm at 24 K. Some energy levels can be formed by the interface between Pt nanoparticles and TiO_2, which also affect the photoelectrochemical properties of Pt/TiO_2 nanocomposite electrodes. The anodic photocurrents at 1.0 V of Pt/TiO_2 nanocomposite electrodes were observed in the visible light range.
© 2001 Elsevier Science B.V. All rights reserved.

Keywords: Pulsed laser deposition; Thin film; Nanocomposite electrode; Photoelectrode

1. Introduction

The size reduction of materials to the nano-meter scale reveals unique physical properties [1]. To use these properties, we must develop the capability to build up tailored nanostructures for a given function by controlling the materials at the molecular level [2,3]. By preparing nanocomposites made of oxide films containing nano-sized semiconductor or metal particles, we can create systems with unusual optical and electrical properties. These include the third order nonlinear optical effects, photoluminescence, selective optical absorption and reflection, and catalytic effects [4–11]. Such unique optical and/or chemical properties result from quantum size effects of the nanoparticles embedded in the matrix and from phenomena occurring at the interface between nanoparticles and matrix [12].

TiO_2 in its anatase form is far less understood than the rutile modification. The rutile form is stable at high temperatures (>700°C) and is usually obtained when pure TiO_2 crystal is synthesized. Recent application of colloidal anatase in novel photochemical solar cells, high mobility n-type charge carriers, and the metal–nonmetal transition in the impurity band of reduced anatase thin films have stimulated interest and investigations [13,14]. Titanium dioxide is a promising photoactive material, though it has a bandgap of 3.2 eV that results in almost no functionality in the visible light range.

The preparation of nanocomposites dispersed with noble metal particles is an approach to overcome such a drawback. Zhao et al. [15] reported that the TiO_2 films containing Au and Ag metal particles also have photosensitivity to visible light, where the anodic photocurrent for oxygen evolution reaction in aqueous solutions can be observed at the wavelengths shorter than 700 nm.

Pt nanoparticles are an effective sensitizer of TiO_2 photocatalysts because of their high catalytic activity and low overpotential for hydrogen evolution reaction. In the decomposition of water in the Pt/TiO_2 system, Pt nanoparticles on TiO_2 can effectively trap the photoexcited electrons in the conduction band of TiO_2, followed by the evolution of hydrogen in aqueous solutions. Pt/TiO_2 composites and nanocomposites have been prepared by a variety of methods such as sol–gel, sputtering, pulsed laser deposition and thermal decomposition methods. Choi et al. [16] investigated the photoelectrochemical properties of Pt/TiO_{2-x} electrodes prepared by thermal oxidation of titanium sheets

* Corresponding author. Tel.: +81-298-61-4896; fax: +81-298-61-6355.
E-mail address: takeshi.sasaki@aist.go.jp (T. Sasaki).

1010-6030/01/$ – see front matter © 2001 Elsevier Science B.V. All rights reserved.
PII: S1010-6030(01)00558-5

followed by the electrodeposition of platinum, where anodic photocurrents were observed only at wavelengths of 200–400 nm. This result was quite different from the Au/TiO_2 and Ag/TiO_2 systems described above.

In this paper, we report the preparation of Pt/TiO_2 nanocomposite thin films by pulsed laser deposition, and the photoelectrochemical properties of these thin films with well-controlled nanostructures in UV–Vis light range. The mechanism of the photoresponse in the visible light of the Pt/TiO_2 nanocomposite thin film electrodes is also discussed.

2. Experimental procedure

2.1. Synthesis of materials

Pt/TiO_2 nanocomposite films were deposited on quartz glass, or indium tin oxide (ITO) glass substrates for photoelectrochemical measurements, by pulsed laser deposition. The mixed pellets of Pt and the TiO_2 were used as the target materials, and the simultaneous ablation of both Pt and TiO_2 components was utilized to deposit the Pt/TiO_2 nanocomposite films. The third harmonic (wavelength = 355 nm) of an Nd:YAG laser was used for the ablation. The laser repetition rate and pulse width were 10 Hz and 7 ns, respectively. The laser light was focused to a 2 mm diameter spot size on the target surface through a lens, and the laser light fluence on the target was varied from 1.7 to 5.7 J/cm^2. The experimental PLD chamber consists of a planetary support system that holds and rotates the target during the ablation process. The target material for the PLD was a mixed pellet of Pt and rutile type TiO_2 (17 mm diameter × 4 mm thick) prepared by the usual ceramic technique. The platinum content in the target was varied from 5 to 20% by weight to obtain films with various Pt content. Anatase form TiO_2 was used for the starting material in order to obtain sufficient target density. Pellets were prepared by pressing and sintering at 900°C for 5 h in air. The thin films were deposited at room temperature on substrates 5.0 cm from the target under a pressure of 1.3 Pa of oxygen for 10 min.

2.2. Materials characterization

All the samples were heated in air at 600°C for crystallization, since the as-deposited films prepared at room temperature were always amorphous. The structures of the films were examined by X-ray diffraction (XRD) analysis using Cu Kα radiation (Rigaku, RAD-C). Nano-scale inhomogeneity and microstructure of the films were analyzed by transmission electron microscope (TEM) observation using JEOL, JEM2000-FXII. The chemical state of Pt, and the Pt/Ti atomic ratio in the nanocomposites were examined by X-ray photoelectron spectroscopy (XPS; PHI, 5600ci). The thickness of the nanocomposite thin films was measured from the edge profile by a surface roughness meter (Tencor Instruments, Alpha-step 3000). The optical transmittance of the nanocomposite films was measured using a spectrometer (Shimadzu, UV-2100PC). Luminescence emission was also measured using a spectrometer (Otsuka Electronics, JMUC-700) with a cryostat (RMC, LTS-22-1) at 24 K in vacuum with an excitation of 325 nm light.

2.3. Photoelectrochemical measurements

The annealed and as-deposited Pt/TiO_2 nanocomposite films on ITO glass substrate were used for photoelectrochemical measurement. The electrical lead wire was attached to the ITO surface by silver paste. The substrates were covered with epoxy resin, except for the nanocomposite and TiO_2 surfaces. A conventional three-electrode system was used in the photoelectrochemical experiments; nanocomposite samples, Pt and Ag/AgCl electrodes were used as working, counter and reference electrodes, respectively. The potential of the working electrode in the electrolyte (0.1 M Na_2SO_4 aqueous solution) was controlled using a potentiostat (Solartron, 1280B). Photocurrents were measured under the irradiation of the light through a monochromator (Shimadzu, SPG-120S) and an electronic shutter (JML Optical Industries, SES-16500) from a 500 W xenon lamp (Ushio, UXL-500D-0).

3. Results and discussion

Fig. 1 shows the Pt/Ti atomic ratio and film thickness of the Pt/TiO_2 nanocomposite films deposited at laser fluences of 5.7, 3.4 and 1.7 J/cm^2 as a function of the Pt content in the

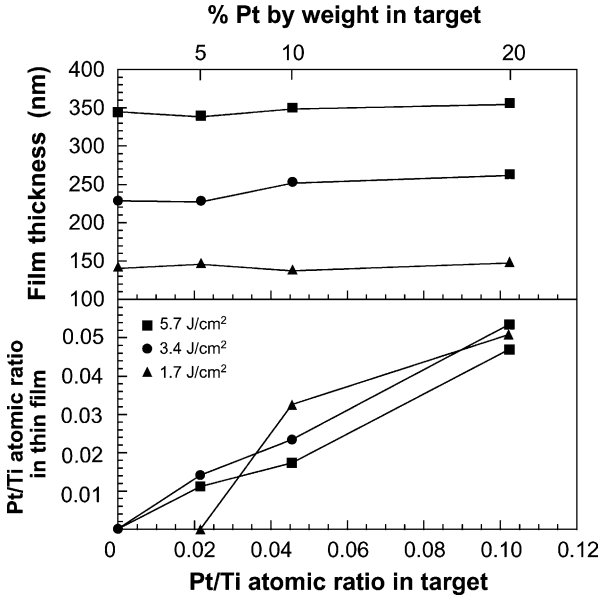

Fig. 1. Pt/Ti atomic ratio and film thickness of the Pt/TiO_2 nanocomposite films deposited at laser fluences of 5.7, 3.4 and 1.7 J/cm^2 as a function of the ratio in the ablation target.

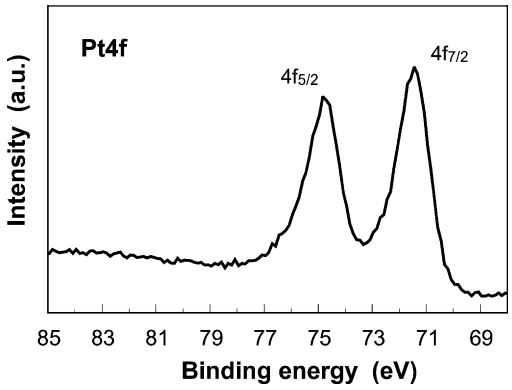

Fig. 2. XPS spectra of Pt 4f levels in the as-deposited film deposited from 20% Pt by weight target at 5.7 J/cm^2.

target. The Pt/Ti atomic ratios in the deposited films are more strongly dependent on the initial content of Pt in the target than on laser fluence. Pt/Ti atomic ratios in the deposited films increased with the platinum content of the targets. The atomic ratios in deposited films were always smaller than those in the target materials. This result could reflect the difference in the ablation threshold of platinum and TiO_2. TiO_2 is more effectively ablated by the laser irradiation than platinum because platinum has a higher ablation threshold than TiO_2 [17]. A tendency for the Pt/Ti atomic ratio to decrease with increasing laser fluence is suggested by the data from 10% Pt by weight target. However experimental uncertainty limits general clarification of this observation in the other targets. In contrast, the film thickness is more strongly dependent on the laser fluence than on the initial Pt content in the target. Film thickness increased only with an increase in the laser fluence under the deposition. Higher fluence can increase the flux of evaporated species from the target materials, resulting in the thicker deposits.

Fig. 2 shows typical XPS spectra of Pt 4f levels in the as-deposited film prepared from 20% Pt by weight target at 5.7 J/cm^2. A binding energy of around 71.4 eV was observed in all of the as-deposited Pt/TiO_2 nanocomposite films, where the Pt/Ti atomic ratio was less than 0.06, indicating that Pt in the nanocomposite films is a metallic state [18]. Platinum was frequently oxidized to PtO or PtO_2 during the deposition when Pt/TiO_2 nanocomposite films were deposited by co-sputtering [12]. Post-annealing of sputtered films was sometimes required to form metallic Pt nanoparticles in such co-sputtered films. For pulsed laser deposition, metallic Pt nanoparticles can easily be obtained in Pt/TiO_2 nanocomposite films without the post-annealing. Fig. 3 shows a typical TEM photograph of the as-deposited Pt/TiO_2 nanocomposite film prepared from 20% Pt by weight target at 5.7 J/cm^2. Dark and bright nanoparticles with diameters of about 30 nm are observed in the photo. The fringe patterns were observed only in a few dark spots, and the spaces in these patterns were estimated to be 2.27 and 2.00–1.92 Å. These values agree well with Pt cubic lattice spaces of (1 1 1) and (2 0 0), respectively [19]. Thus,

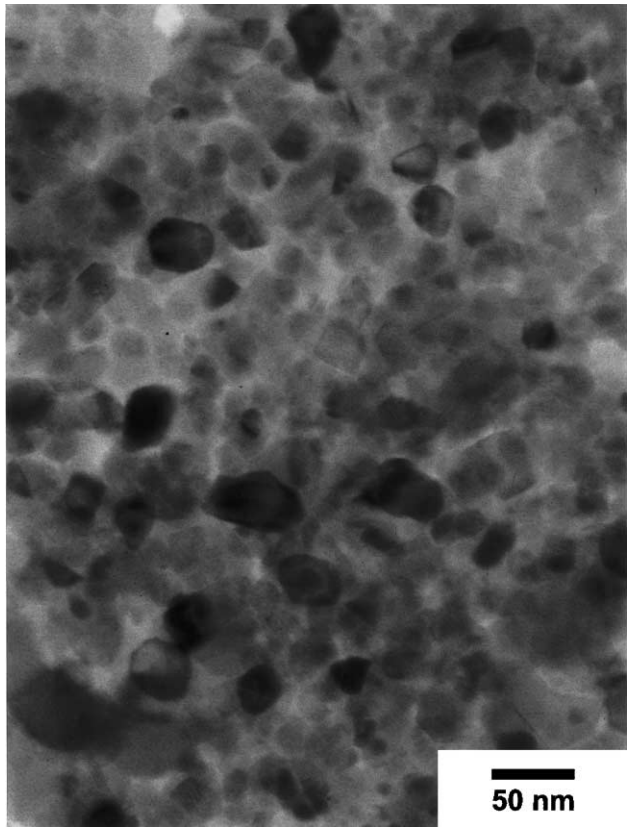

Fig. 3. TEM photograph of the as-deposited Pt/TiO_2 nanocomposite film prepared from 20% Pt by weight target at 5.7 J/cm^2.

the dark nanoparticles in Fig. 3 represent Pt nanoparticles. After the samples were heated, the structure dramatically changed to be needle-like structures of ~2 μm in length associated with Pt nanoparticles.

Fig. 4 shows typical XRD patterns of heated TiO_2 and Pt/TiO_2 nanocomposite thin films at 600°C prepared at 5.7 J/cm^2 from pure TiO_2 and 20% Pt by weight targets, respectively. All of the as-deposited films looked like amorphous because no diffraction peak was observed. In Fig. 4

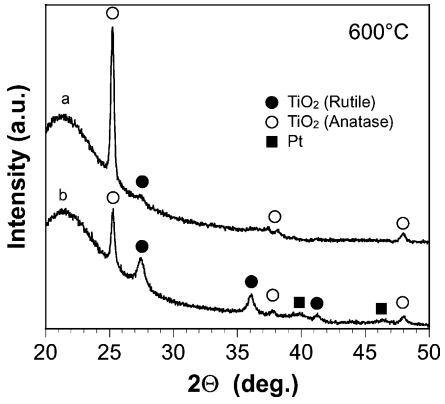

Fig. 4. XRD patterns of heated TiO_2 (a) and Pt/TiO_2 nanocomposite (b) films at 600°C prepared from pure TiO_2 and 20% Pt by weight targets at 5.7 J/cm^2.

the XRD pattern of the Pt/TiO_2 nanocomposite films shows that the predominant crystal phase is anatase TiO_2. However, rutile TiO_2 phase is also observed. It should be noted that crystal rutile peaks are broader than the anatase, indicating smaller particle dimensions. The very broad peak of crystal Pt is observed near $2\theta = 40^\circ$. The breadth of this peak is characteristic of Pt nanocrystals, as observed in the Pt/TiO_2 nanocomposite films deposited by sputtering [12]. The crystallite size of Pt in the heated Pt/TiO_2 nanocomposite film prepared from 20% Pt by weight target at 5.7 J/cm^2 was roughly estimated to be about 40 nm using the XRD peak width. It should be noted that the heated TiO_2 film prepared from pure TiO_2 target at 5.7 J/cm^2 is more than 95% anatase phase. It was observed that as the laser fluence decreased, the ratio of anatase to rutile TiO_2 decreased in all samples containing Pt. No crystalline Pt peaks are discernable from the background in samples prepared from 5 and 10% Pt by weight targets.

In order to estimate the optical bandgap of the films, the UV–Vis spectra of samples were recorded. The as-deposited films are almost completely absorptive, resulting from TiO_2 defects, which can be removed by annealing. Fig. 5 shows the UV–Vis spectra of the heated Pt/TiO_2 nanocomposite films and TiO_2 films prepared from targets with different Pt contents at 5.7 J/cm^2. The variation in the absorption coefficient with photon energy for direct allowed band-to-band transition can be represented as

$$a^2 = a_0^2(h\nu - \Delta E)$$

where a is the absorption coefficient and ΔE is the bandgap [20]. After correcting for reflection losses, the optical bandgap can be estimated by extrapolating the linear portion of the curve to $a^2 = 0$. For the pure TiO_2 film, we obtain a value of $\Delta E = 3.15$ eV. The bandgaps of Pt/TiO_2 nanocomposite films prepared from 5, 10 and 20% Pt by weight targets were estimated to be 2.9, 2.8 and 2.3 eV, respectively. In addition, luminescence emission was observed by UV irradiation at 680–800 nm only from Pt/TiO_2

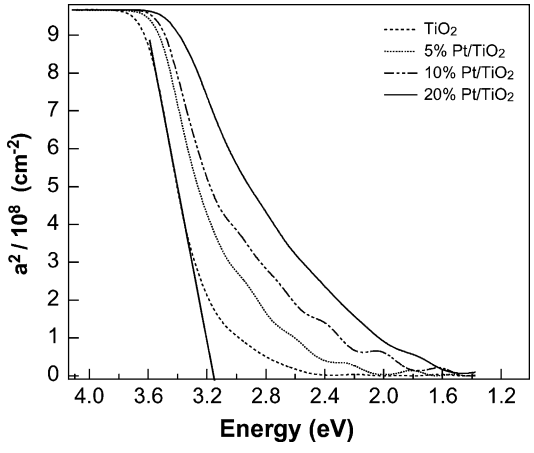

Fig. 5. UV–Vis spectra of the heated Pt/TiO_2 nanocomposite films and TiO_2 films prepared from targets with different Pt contents at 5.7 J/cm^2.

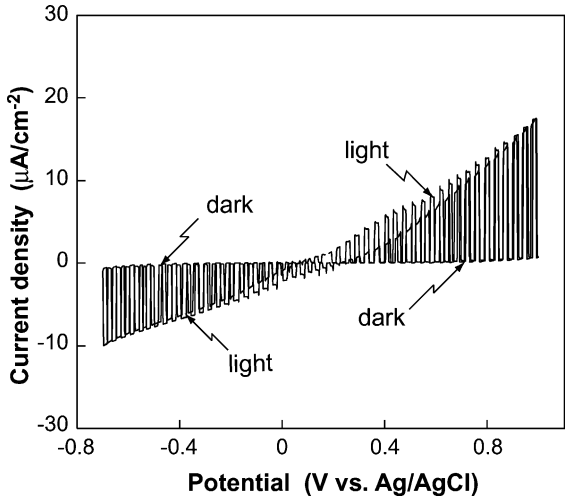

Fig. 6. Cyclic voltammogram of the heated Pt/TiO_2 nanocomposite electrode which was prepared from 5% Pt by weight target at 5.7 J/cm^2.

nanocomposite films at 24 K. These results suggest that the some energy levels could be formed in the bandgap of TiO_2. Thus, the photoexcitation of electrons in Pt/TiO_2 nanocomposite films needs only lower energy than the bandgap energy of TiO_2. We expected that photoelectrochemical properties of Pt/TiO_2 nanocomposite electrodes would be completely different from those of pure TiO_2 electrodes, and that the former should have a photoresponse in the visible light range.

Indeed, the photoelectrochemical properties of Pt/TiO_2 nanocomposite electrodes were completely different from those of TiO_2 electrodes. Fig. 6 shows a typical cyclic voltammogram of the heated Pt/TiO_2 nanocomposite electrode prepared from 5% Pt by weight target at 5.7 J/cm^2. The heated and as-deposited Pt/TiO_2 nanocomposite electrodes have almost the same behavior. Under anodic polarization with the irradiation of the total light from a Xe lamp, anodic photocurrents for the oxygen evolution reaction were observed at potentials above 0.2 V. The anodic photocurrents of all the nanocomposite electrodes were smaller than those of pure TiO_2 electrodes. Cathodic photocurrents were also observed in all nanocomposite electrodes. These photocurrents increased in the solution under oxygen bubbling rather than nitrogen bubbling, indicating that the cathodic photocurrent can be ascribed to the reduction of oxygen by photoexcited electrons.

Fig. 7 shows the anodic photocurrent at 1.0 V for Pt/TiO_2 nanocomposite electrodes prepared from 5 and 20% Pt by weight target as a function of the irradiating light wavelength. The photocurrents of as-deposited nanocomposite electrodes were higher than those of heated electrodes. This trend was the same as the cyclic voltammogram of all samples. Many defects in as-deposited samples could affect the electrical conductivities, resulting in the higher photocurrent. However, the anodic photocurrent of as-deposited electrodes was a little unstable. It should be noted that the

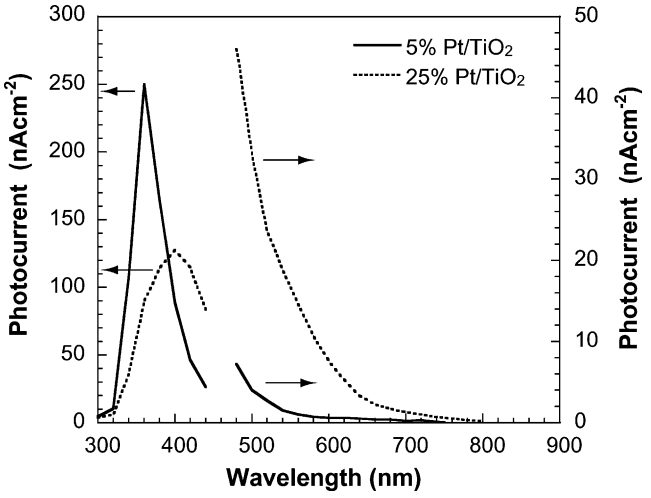

Fig. 7. Anodic photocurrent of Pt/TiO_2 nanocomposite electrodes at 1.0 V vs. Ag/AgCl as a function of the irradiating light wavelength. Pt/TiO_2 nanocomposite electrodes were prepared from 5 and 20% Pt by weight target at 5.7 J/cm^2.

anodic photocurrents in the wavelength region from 450 to 750 nm were clearly observed in the Pt/TiO_2 nanocomposite electrodes prepared from 20% Pt by weight target. This photon energy range is smaller than the bandgap energy of TiO_2, indicating the existence of some energy levels in the optical bandgap of TiO_2 that contribute to the photoresponse in visible light. These results are very consistent with the UV–Vis and luminescence emission measurements stated in the previous section. The anodic photocurrent in visible light is higher in the Pt/TiO_2 nanocomposite film prepared from 20% than 5% Pt by weight target. Metallic Pt nanoparticles exist in the heated Pt/TiO_2 nanocomposite films prepared from 20% Pt by weight target, as previously stated. These results suggest that the metallic Pt nanoparticles could play an important role in creating energy levels in the bandgap.

It is well known that a Schottky barrier is formed at the interface between a metal and semiconductor. The barrier height of the Pt–TiO_2 interface is estimated to be 1.64 eV from the work function of Pt (5.64 eV) [21] and the electron affinity of TiO_2 (4.0 eV) [15]. The photoexcitation of electrons from the Pt metal to the conduction band of TiO_2 could take place under the irradiation of light with energy exceeding 1.64 eV. As shown in Fig. 7, the anodic photocurrent is clearly observed at wavelengths shorter than 750 nm. These energy levels are a very reasonable energy range for the electron excitation from Pt to TiO_2.

It should be noted that the Pt nanoparticles are isolated in Pt/TiO_2 nanocomposite films, indicating that each Schottky barrier between Pt nanoparticles and TiO_2 is localized in the TiO_2 matrix. The number density of such localized interfaces can also be important for the total photoresponse of Pt/TiO_2 nanocomposite films. A high number density of Pt nanoparticles in TiO_2 allows producing an efficient electronic state density of the energy levels, which can contribute to the photoexcitation with lower energy than that of the bandgap of TiO_2, resulting in a unique photoresponse in visible light.

Attempts to extend the photoresponse of TiO_2 towards visible light have been studied for both photocatalysis and photovoltaic cell applications by several methods, such as the addition of cationic dopants into TiO_2 [22] and dye coatings on the TiO_2 surface [23]. The Pt/TiO_2 nanocomposite electrodes also have photoresponse to visible light, which indicates a new possibility for improving TiO_2 photoresponse.

4. Conclusions

Pt/TiO_2 nanocomposite films were prepared from mixture targets of Pt and TiO_2 by pulsed laser deposition. The Pt/Ti atomic ratio in films was controlled by the initial content of Pt in the target, and was independent of laser fluence. It is inferred from TEM, XPS and XRD measurements that as-deposited Pt/TiO_2 nanocomposite films are composed of metallic Pt nanoparticles with diameters of about 30 nm and an amorphous TiO_2 matrix, which are crystallized into the dominant crystal structure of anatase phase after heating at 600°C. The optical bandgap of Pt/TiO_2 nanocomposite films was less than 2.3 eV, and a photoluminescence emission between 680 and 800 nm at 24 K was observed. The anodic photocurrents of Pt/TiO_2 nanocomposite electrodes at 1.0 V were also observed in visible light. Some energy levels can be formed by the interface between Pt nanoparticles and TiO_2, which also affect both the photoelectrochemical and optical properties of Pt/TiO_2 nanocomposite films. The localized Schottky barrier at the interface between Pt nanoparticles and TiO_2 could contribute to the photoresponse in the visible light range.

Acknowledgements

This study was financially supported by the Center of Excellence (COE) project from the Science and Technology Agency (STA) of Japan. This work was partially performed while Kenneth M. Beck visited Tsukuba, supported by STA and COE research fellowships.

References

[1] Y.M. Chiang, J. Electroceram. 1 (1997) 205.
[2] M.C. Roco, J. Nanoparticle Res. 1 (1999) 1.
[3] E.L. Hu, D.T. Shaw, in: R.W. Siegel, E.L. Hu, M.C. Roco (Eds.), Nanostructure Science and Technology, Kluwer Academic Publishers, Dordrecht, 1999, pp. 15–33.
[4] D. Ricard, Ph. Roussignol, Ch. Flytzanis, Opt. Lett. 10 (1985) 511.
[5] Y. Maeda, N. Tsukamoto, Y. Yazawa, Y. Kanemitsu, Y. Masumoto, Appl. Phys. Lett. 59 (1991) 3168.
[6] J. Papp, H.S. Shen, R. Kershaw, K. Dwight, A. Wold, Chem. Mater. 5 (1993) 222.
[7] S. Hayashi, M. Kataoka, K. Yamamoto, Jpn. J. Appl. Phys. 32 (1993) L274.

[8] T. Kineri, M. Mori, K. Kadono, T. Sakaguchi, M. Miya, H. Wakabayashi, T. Tsuchiya, J. Ceram. Soc. Jpn. 101 (1993) 1340.
[9] H. Kozuka, G. Zhao, S. Sakka, J. Sol–Gel Sci. Technol. 2 (1994) 741.
[10] S. Yoshida, T. Hanada, S. Tanabe, N. Soga, Jpn. J. Appl. Phys. 35 (1996) 2694.
[11] F. Hache, D. Ricard, Ch. Flytzanis, U. Kreigig, Appl. Phys. A 47 (1998) 347.
[12] T. Sasaki, N. Koshizaki, S. Terauchi, H. Umehara, Y. Matsumoto, M. Koinuma, Nanostruct. Mater. 8 (1998) 1077.
[13] S.-D. Mo, W.Y. Ching, Phys. Rev. B 51 (1995) 13023.
[14] H.-A. Durand, J.-H. Brimaud, O. Hellman, H. Shibata, S. Sakuragi, Y. Makita, D. Gesbert, P. Meyrues, Appl. Surf. Sci. 86 (1995) 122.
[15] G. Zhao, H. Kozuka, T. Yoko, Thin Solid Films 277 (1996) 147.
[16] Y.K. Choi, S.S. Seo, K.H. Chjo, Q.W. Choi, S.M. Park, J. Electrochem. Soc. 139 (1992) 1803.
[17] D.B. Chrisey, G.K. Huber (Eds.), Pulsed Laser Deposition of Thin Films, Wiley, New York, 1994, p. 455.
[18] M. Davidson, G. Hofiund, L. Niinisto, H. Laitinen, J. Electroanal. Chem. 228 (1987) 471.
[19] CAS #7440-06-04, $d = 2.265$ Å as prepared at NBS, Gaitherburg, MD.
[20] A.K. Abass, A.K. Hasen, R.H. Misho, J. Appl. Phys. 58 (1985) 1640.
[21] H.B. Michaelson, J. Appl. Phys. 48 (1977) 4729.
[22] H. Yamashita, Y. Ichihashi, M. Takeuchi, S. Kishiguchi, M. Anpo, J. Synchrotron Radiat. 6 (1999) 451.
[23] B. O'Regan, M. Grätzel, Nature 353 (1991) 737.